Radiocarbon (2025), pp. 1–16
doi:10.1017/RDC.2024.118

CAMBRIDGE UNIVERSITY PRESS

RESEARCH ARTICLE

Monsoon-regulated marine carbon reservoir effect in the northern South China Sea

Ling Yang[1,2,3], Weijian Zhou[1,2,4], Peng Cheng[1,2], Luyuan Zhang[1,2], Gangjian Wei[5], Xiaolin Ma[1], Jie Zhou[6], Hong Yan[1,4], Ning Chen[1,2] and Yaoyao Hou[1,2]

[1]State Key Laboratory of Loess, Institute of Earth Environment, Chinese Academy of Sciences, Xi'an, 710061, China, [2]Shaanxi Key Laboratory of Accelerator Mass Spectrometry Technology and Application, Xi'an AMS Center of IEECAS, 710061, China, [3]University of Chinese Academy of Sciences, Beijing, 100049, China, [4]Laoshan Laboratory, Qingdao, 266237, China, [5]State Key Laboratory of Isotope Geochemistry, Guangzhou Institute of Geochemistry, Chinese Academy of Sciences, Guangzhou, 510640, China and [6]Xi'an institute for innovative Earth Environment Research, Xi'an 710061, China
Corresponding author: Weijian Zhou; Email: weijian@loess.llqg.ac.cn

Received: 01 February 2024; **Revised:** 01 August 2024; **Accepted:** 14 August 2024

Keywords: Asian Monsoon; coral; marine radiocarbon reservoir effect; pre-bomb; South China Sea

Abstract
The ubiquitous marine radiocarbon reservoir effect (MRE) constrains the construction of reliable chronologies for marine sediments and the further comparison of paleoclimate records. Different reference values were suggested from various archives. However, it remains unclear how climate and MREs interact. Here we studied two pre-bomb corals from the Hainan Island and Xisha Island in the northern South China Sea (SCS), to examine the relationship between MRE and regional climate change. We find that the MRE from east of Hainan Island is mainly modulated by the Southern Asian Summer Monsoon-induced precipitation (with 11.4% contributed to seawater), rather than wind induced upwelling. In contrast, in the relatively open seawater of Xisha Island, the MRE is dominated by the East Asian Winter Monsoon, with relatively more negative (lower) ΔR values associated with high wind speeds, implying horizontal transport of seawater. The average SCS ΔR value relative to the Marine20 curve is –161±39 ^{14}C years. Our finding highlights the essential role of monsoon in regulating the MRE in the northern SCS, in particularly the tight bond between east Asian winter monsoon and regional MRE.

Introduction

Marine sediments play an important role in interpreting past climate change which provides a crucial clue for future climate forecasting (Lisiecki and Raymo 2005; Tierney et al. 2020; Wang et al. 2014). Previous studies based on foraminifera, bivalve, and coral have made excellent progress in revealing the past climate change (Yan et al. 2017; Yu 2012; Zhang et al. 2021). However, the ambiguous nature of the marine radiocarbon reservoir effect (MRE) constrains the building of reliable chronology (Alves et al. 2018; Burr et al. 2009; Stuiver et al. 1986), thus hindering the reconstruction and comparison of these centennial to millennial scale climate changes. Hence, precisely evaluating temporal and spatial MRE variations is urgently needed in paleoclimate research.

MREs often reflect air-sea exchange, regional ocean circulation, and freshwater input (Stuiver and Ostlund 1983; Southon et al. 2002). A MRE can be expressed as the radiocarbon age difference between the atmosphere and the surface ocean. This difference is expressed as the value R (reservoir age) in radiocarbon years. Generally, MREs are cited as ΔR values, which are differences between measured R values and modeled R values (e.g. difference between IntCal13 and Marine13 calibration curves) for a particular region, based on calibration curves (e.g. Marine 13, Reimer et al. 2013).

Corals loyally document the ^{14}C of seawater dissolved inorganic carbon (DIC) (Druffel 1997; Grumet et al. 2004) and can be accurately dated by U-series (Yu et al. 2006) or absolutely refined annual band, which provide the opportunity for evaluating ΔR. A series of studies have determined regional

R and ΔR based on corals or known-age materials (Burr et al. 2009; Oliveira et al. 2019; Yoneda et al. 2007). However, R and ΔR are seen to vary with time in coral records (Hua et al. 2015; Yu et al. 2010) and model results (Butzin et al. 2017). Hence R and ΔR are a function of time and location. Previous studies have revealed a tight connection between seawater ^{14}C and climate from pre- and post-bomb corals (Grottoli et al. 2003; Hirabayashi et al. 2017). Nevertheless, the temporal relationship between regional ΔR and climate change for most regions remains unknown.

As the largest marginal sea in the Pacific, with abundant riverine sediments and a high sedimentation rate, the monsoon-dominated South China Sea (SCS) has been a focus of paleoclimate research (e.g. Shen et al. 2022; Wang et al. 2014). A precise ΔR for the SCS and its temporal variability are of importance for elucidating these paleoclimate records. Previous studies have suggested different ΔR values for the SCS. For instance, ΔR at Hòn Tre Island, Vietnam (Bolton et al. 2016), was estimated to be 18±29 ^{14}C years (relative to Marine 13, Reimer et al. 2013), larger than the ΔR at Con Dao Island (Dang et al. 2004) of –74±39 ^{14}C years (relative to Marine 98, Stuiver et al. 1998) and the average ΔR (Southon et al. 2002) of –25±20 ^{14}C years for the SCS (relative to Marine 98, Stuiver et al. 1998). Nevertheless, decadal ΔR variations related to climate have yet to be determined. Furthermore, the newly updated marine calibration curve (Marine20 curve) (Heaton et al. 2020), is almost 150 ^{14}C years older than that implied by the Marine13 (Reimer et al. 2013) and previous marine curves. Hence, it is crucial to reconcile regional ΔR time series records to clarify the relationship between ΔR and climatic factors through time.

In this study, we present two coral radiocarbon records exceeding two decades from the east of Hainan Island and Xisha Island in the northern SCS. The relationship between regional ΔR and climatic factors (e.g. monsoon) in these corals were thoroughly examined and explored. Further, the newly average ΔR for the SCS base on the most recent marine radiocarbon Curve-Marine20 (Heaton et al. 2020) and its implication for paleoclimate research were specifically considered.

Materials and methods

Oceanographic setting of the SCS

As a semi-closed marginal sea, the SCS connects the surrounding sea through seven straits. The Luzon strait, contributes to the primary water exchange with the northwest Pacific Ocean (Qu et al. 2009), with a deep sill of 2400m (Qu et al. 2006). In addition, two large rivers, the Pearl River and Mekong River, supply a large amount of sediments into the north SCS and west SCS, with annual runoffs of 3.3 and 4.7×10^{11} m^3, respectively (Mckee et al. 2004). The surface circulation in the SCS seasonally shifts due to the reversing monsoon winds, with clockwise flows in summer and anti-clockwise flows in winter (Hu et al. 2000). Moreover, the summer monsoon influences coastal upwelling prevails around east of Hainan, off Vietnam and off Guangdong province, while the prevalent coastal upwelling west of Luzon is in winter under the effect of winter monsoon (Wu and Li 2003; Hu and Wang 2016).

The summer sea surface temperature (SST) in the SCS is roughly homogeneous above 28°C. In contrast, the winter SST displays conspicuous ascent from north to south (Figure 1 a–d). These seasonal differences in SST distribution patterns are mainly induced by seasonal reversing monsoon including the East Asian Winter Monsoon (EAWM) and the Southern Asian Summer Monsoon (SASM) (Liu et al. 2004). In this study, the two sample sites (shown in Figure 1 a and b) share distinct oceanography. At east of Hainan Island, prevailing in summer, the prominent upwelling dominant the regional circulation, which is mainly influenced by the SASM (Hu and Wang 2016; Jing et al. 2009). During summer, shallow regional mixed layer depth is observed (Figure 1 e) (Zeng et al. 2016), which favors upwelling of aged ^{14}C to the surface. In contrast, at Xisha Island, an open ocean site, no seasonal upwelling is observed (deep mixed layer depth, Figure 1 f). The annual average wind speed is larger in Xisha Island than in Hainan Island, especially in winter (Figure 1 g and h). Besides, runoff from the

https://doi.org/10.1017/RDC.2024.118 Published online by Cambridge University Press

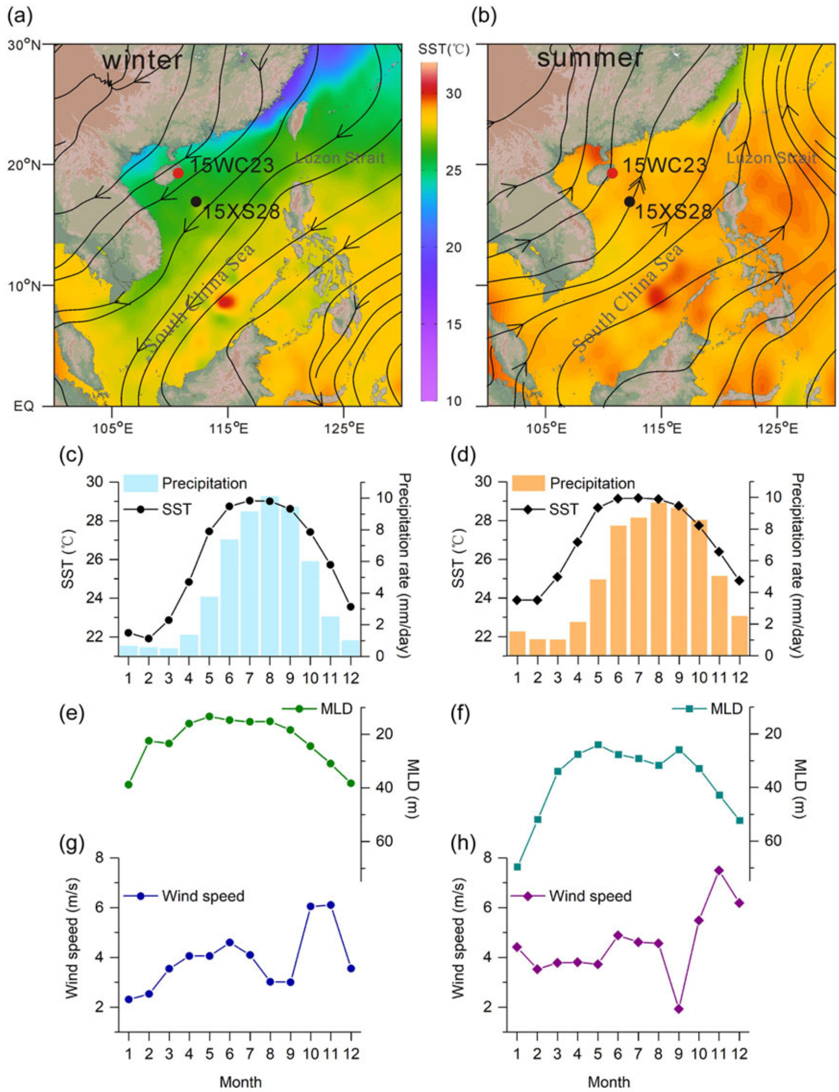

Figure 1. *Map and hydroclimate parameters of sampling site. (a) winter (December-January-February) and (b) summer (June-July-August) mean 850 hPa stream line from the ERA-Interim (https://climatedataguide.ucar.edu/climate-data/era-interim-derived-components), the red and black dots represent the sampling sites of coral core 15WC23 and 15XS28 from east of Hainan Island and Xisha Island, respectively. (c) Monthly mean sea surface temperature (SST), precipitation and (g) wind speed at east of Hainan Island (centered at 19°N, 110°E within 2° × 2° grid) from NCEP Reanalysis Dataset (https://psl.noaa.gov/cgi-bin/data/timeseries/timeseries1.pl). (d) Monthly mean sea surface temperature (SST), precipitation and (h) wind speed at Xisha Island (centered at 17°N, 112°E within 2° × 2° grid) from NCEP Reanalysis Dataset. All the monthly mean data are ranged from 1948 to 2021. (e) and (f) Monthly mean mixed layer (MLD) depth from SCSPOD14 (Zeng et al. 2016) ranging from 1971 to 2015 at east of Hainan Island (centered at 19.5°N, 111°E within 0.5° × 0.5° grid) and Xisha Island (centered at 17°N, 112.5°E within 0.5° × 0.5° grid), respectively.*

https://doi.org/10.1017/RDC.2024.118 Published online by Cambridge University Press

Wanquan River and Wenjiao River at Hianan Island accounts for more than 6×10^9 m^3 yr^{-1} (Zhang et al. 2013), while negligible runoff occurs at the Xisha Island.

Sampling

In 2015, two coral cores were obtained from living massive *Porites lutea* colonies from the northern SCS. The coral core 15WC23 (19.39°N, 110.76°E) was collected at a water depth of 5 m, from a fringing reef, off the east coast of Hainan Island (Figure 1 a and b, red dot). The other coral core 15XS28 (16.96°N, 112.25°E) was collected at a water depth of 4 m from Qilianyu Reef in the Xisha Islands (Figure 1 a and b, black dot). The chronology of the coral cores was well established by the annual density bands revealed by X-ray photograph (Figure S1, see Supplementary), with a growth period from 1900 to 2015 for 15WC23 (Chen et al. 2021) and from 1930 to 2015 for 15XS28 (Kang et al. 2021). The powder samples were carefully milled along the main growth axis by a digitally controlled milling machine (Deng et al. 2013). Limited by sample size, coral 15WC23 and 15XS28 were sampled with biennial and annual resolution, respectively.

Radiocarbon dating

All pre-1950 powder samples (45 samples in total) were employed for radiocarbon analysis. For each sample, about five to seven milligrams of coral powder were reacted with 85% phosphoric acid in a Y-shaped vessel under vacuum of less than 1×10^{-1} torr. After complete reaction, the CO_2 gas was purified in a vacuum line and reduced to graphite using a zinc reduction method (Slota et al. 1987). Graphite samples were then measured for ^{14}C analysis at the Xi'an Accelerator Mass Spectrometry (AMS) center (Zhou et al. 2016).

Result

The radiocarbon result (Table 1) of 45 coral samples is presented in Figure 2, expressed as ΔR. The ΔR data from east Hainan Island from 1900 to 1949 are cited with biennial resolution, while the Xisha Island results from 1930 to 1949 are cited with annual resolution. Recalculated previous-published average ΔR values from different sites around the SCS are summarized in Table 2, consisting of 725 ΔR values from eighteen sites. The R, ΔR and the associated $\Delta^{14}C$ are calculated by the following equations (Stuiver et al. 1986; Stuiver and Polach 1977):

$$\text{Measured R(t)} = \text{Measured } ^{14}\text{C age(t)} - \text{Terrestrial } ^{14}\text{C age(t)} \tag{1}$$

$$\Delta\text{R(t)} = \text{Measured R(t)} - \text{modeled R(t)} \tag{2}$$

$$\text{Modeled R(t)} = \text{Modeled marine } ^{14}\text{C age(t)} - \text{Terrestrial } ^{14}\text{Cage(t)} \tag{3}$$

$$\text{Measured } ^{14}\text{C age(t)} = -8033 \times \ln(F) \tag{4}$$

$$\Delta^{14}\text{C} = Fe^{\lambda(1950-t)-1} \times 1000‰ \tag{5}$$

Where t is the true living age of the sample in cal BP (based on the counted annual density band), F represents the fraction of Modern carbon, $\lambda = 1/8267$ yr^{-1} is the radiocarbon decay constant associated with a 5730-yr half-life, and t is the calendar age of the sample (Stuiver and Polach 1977). The terrestrial and modeled ^{14}C age were obtained from Intcal20 Curve and Marine20 Curve, respectively.

https://doi.org/10.1017/RDC.2024.118 Published online by Cambridge University Press

Table 1. *ΔR result from east of Hainan Island and Xisha Island*

			East of Hainan Island (19.39°N, 110.76°E)					
Lab number	Sample number	True age	*F* value	Error	^{14}C age (BP)	Error (y)	ΔR	Error
XA52553	WC-34	1948	0.9519	0.0016	396	13	–208	13
XA53923	WC-35	1946	0.9513	0.0017	401	15	–203	15
XA52567	WC-36	1944	0.9532	0.0015	385	13	–219	13
XA53921	WC-37	1942	0.9474	0.0020	434	17	–170	17
XA52551	WC-38	1940	0.9492	0.0015	419	13	–185	13
XA53922	WC-39	1938	0.9522	0.0017	393	15	–211	15
XA52566	WC-40	1936	0.9504	0.0016	408	14	–196	14
XA53919	WC-41	1934	0.9460	0.0016	446	14	–158	14
XA52552	WC-42	1932	0.9496	0.0015	416	13	–188	13
XA53920	WC-43	1930	0.9518	0.0018	397	15	–207	15
XA52565	WC-44	1928	0.9540	0.0019	379	16	–226	16
XA53918	WC-45	1926	0.9490	0.0024	421	21	–184	21
XA52550	WC-46	1924	0.9501	0.0016	412	13	–193	13
XA53917	WC-47	1922	0.9487	0.0016	423	14	–182	14
XA52564	WC-48	1920	0.9520	0.0017	395	15	–210	15
XA53916	WC-49	1918	0.9467	0.0018	440	15	–165	15
XA52549	WC-50	1916	0.9491	0.0015	420	13	–185	13
XA53915	WC-51	1914	0.9426	0.0016	475	14	–131	14
XA52563	WC-52	1912	0.9541	0.0017	378	14	–229	14
XA53914	WC-53	1910	0.9452	0.0017	452	14	–155	14
XA52548	WC-54	1908	0.9500	0.0016	412	14	–196	14
XA53913	WC-55	1906	0.9487	0.0015	423	13	–186	13
XA52562	WC-56	1904	0.9510	0.0015	403	13	–208	13
XA53912	WC-57	1902	0.9457	0.0016	448	14	–164	14
XA52547	WC-58	1900	0.9483	0.0017	427	14	–186	14

			Xisha Island (16.96°N, 112.25°E)					
Lab number	Sample number	True age	*F* value	Error	^{14}C age (BP)	Error (y)	ΔR	Error
XA53632	XS-66	1949	0.9521	0.0018	394	15	–210	15
XA53631	XS-67	1948	0.9451	0.0021	454	18	–150	18
XA53633	XS-68	1947	0.9485	0.0021	425	18	–179	18
XA52580	XS-69	1946	0.9537	0.0018	381	15	–223	15
XA53630	XS-70	1945	0.9510	0.0019	404	16	–200	16
XA53627	XS-71	1944	0.9504	0.0022	409	18	–195	18
XA53628	XS-72	1943	0.9492	0.0017	419	15	–185	15
XA52579	XS-73	1942	0.9545	0.0020	374	17	–230	17
XA53629	XS-74	1941	0.9518	0.0020	397	17	–207	17
XA53626	XS-75	1940	0.9511	0.0017	403	15	–201	15
XA53625	XS-76	1939	0.9519	0.0019	396	16	–208	16
XA52576	XS-77	1938	0.9507	0.0015	407	13	–197	13
XA52603	XS-78	1937	0.9528	0.0021	388	18	–216	18
XA52602	XS-79	1936	0.9496	0.0018	416	15	–188	15
XA52601	XS-80	1935	0.9506	0.0018	407	15	–197	15
XA52575	XS-81	1934	0.9500	0.0016	412	14	–192	14
XA52600	XS-82	1933	0.9521	0.0021	394	18	–210	18
XA52599	XS-83	1932	0.9527	0.0018	389	15	–215	15
XA52598	XS-84	1931	0.9509	0.0019	404	16	–200	16
XA52574	XS-85	1930	0.9519	0.0017	396	15	–209	15

https://doi.org/10.1017/RDC.2024.118 Published online by Cambridge University Press

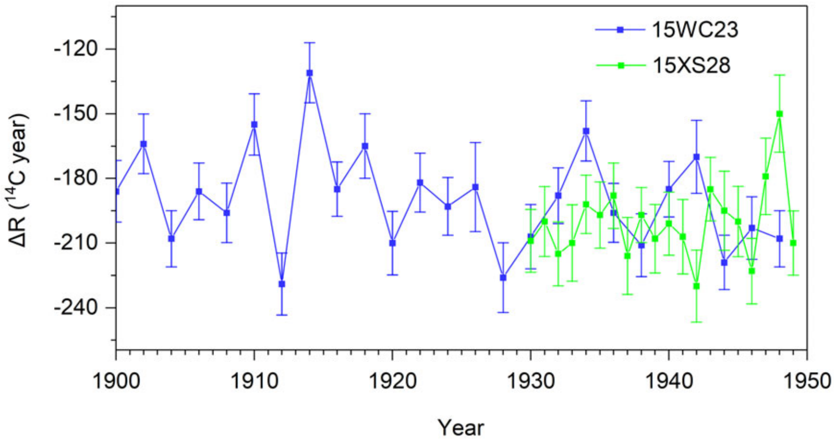

Figure 2. *The ΔR result from east of Hainan Island (15WC23, blue dotted line) and Xisha Island (15XS28, green dotted line).*

ΔR results from Hainan Island and Xisha Island

As shown in Figure 2, 25 ΔR results from east of Hainan Island (blue dotted line) fluctuate from –229 ±14 to –131±14 ^{14}C years (average value –190±23 ^{14}C years) from 1900 to 1949. Additionally, 20 ΔR data from Xisha Island (green dotted line) range from –230±17 to –150±18 ^{14}C years (average value –201±16 ^{14}C years) from 1930 to 1949. Generally, our sites have more negative average ΔR values than other SCS sites (Table 2, published ΔR values were all recalculated using Marine20), except for Con Dao Island, Vietnam (–226±18 ^{14}C years) (Dang et al. 2004; Mitsuguchi et al. 2007) and Janao Bay, Philipines (–216±50 ^{14}C years) (Southon et al. 2002). Additionally, the average Hainan Island ΔR value is lower than that off Hòn Tre Island, Vietnam (–135±12 ^{14}C years) (Bolton et al. 2016; Goodkin et al. 2019), although upwelling occurs at both sites.

Averaged ΔR for the SCS

As summarized in Table 2, overall 725 ΔR values from 18 sites were compiled to recalculate the regional ΔR around the SCS ranging from 1900 to 1950. The majority of ΔR values were obtained from the coral skeletons. Twelve sites and 130 ΔR values in total were included within the SCS. The updated SCS ΔR values varied from –61±14 ^{14}C years to –241±40 ^{14}C years, with the maximum ΔR value from Houbihu, Nanwan Bay, Taiwan, and the minimum ΔR from Con Dao Island, Vietnam. The average SCS ΔR is –161±39 ^{14}C years. Note that the average value and error were calculated by the formulas from http://calib.org/marine/AverageDeltaR.html.

Discussion

ΔR is mainly regulated by the regional upwelling, freshwater input, and the circulation (Stuiver and Ostlund 1983). Normally, areas with notable upwelling have high ΔR values, and areas with more freshwater have relatively low ΔR values. The effect of surface circulation on ΔR depends on the Δ^{14}C value upstream of the site. Besides, the decreasing atmospheric Δ^{14}C (Suess effect, Suess 1955) since the industrial revolution probably influence our ΔR calculation. However, given the ambiguous trend of ΔR at the Hainan Island and long equilibration times (~10 yr) between atmosphere and ocean (Bolton et al. 2016), we believed negligible impact of the Suess effect on our coral Δ^{14}C. Moreover, the Suess effect was ignored at Marine20 calibrated curve (Heaton et al. 2020), by its nonsignificant statistics. Therefore, we neglected potential influence from the Suess effect. As mentioned above, the ΔR

https://doi.org/10.1017/RDC.2024.118 Published online by Cambridge University Press

Table 2. *The detailed information of collected and recalculated ΔR data around the SCS*

Longitude	Latitude	Area	Range (year)	Type	Number	Average ΔR (^{14}C year)	Error	Reference
Within the SCS								
109.3	12.21	Near Hòn Tre Island, Vietnam	1900–1949	Coral	100	–135	12	Bolton et al. 2016; Goodkin et al. 2019
112.3	16.7	Xisha island	1905–1948	Coral	3	–136	47	Southon et al. 2002
112.25	16.96	Xisha island	1930–1949	Coral	20	–201	16	This study
120.7	21.9	Houbihu Island	1942–1945	Coral	2	–76	98	Ramos et al. 2019
120.48	17.98	Currimao Coast	1945–1949	Coral	10	–142	38	Hirabayashi et al. 2019
119.01	11.48	Palawan island	1947–1949	Coral	13	–108	16	Wu and Fallon 2020
106.55	8.66	Con Dao, Vietnam	1948–1949	Coral	2	–226	16	Mitsuguchi et al. 2007; Dang et al. 2004
110.76	19.39	Wenchang, Hainan Island	1900–1949	Coral	25	–190	23	This study
120.5	12.5	Mindoro Strait, Philippines	1908	Bivalve	1	–69	71	Southon et al. 2002
120.9	13.8	Janao Bay, Luzon, Philippines	1916	Gastropod	1	–216	50	Southon et al. 2002
99.7	9.6	Ko Ang Trang, Thailand	1923	Gastropod	1	–175	71	Southon et al. 2002
106.8	10.8	Saigon	1945	Bivalve	1	–164	57	Southon et al. 2002
103.8	2.9	Singapore	1945	Bivalve	1	–156	39	Southon et al. 2002
Outside the SCS								
122.2	18.5	Palaui Island	1945–1948	Coral	2	–99	105	Ramos et al. 2019
119.06	5.03	Langkai Island	1900–1949	Coral	451	–129	34	Fallon and Guilderson 2008
134.25	7.28	Palau Archipelago	1945–1949	Coral	5	–154	21	Glynn et al. 2013
124	24	Ishigaki Island	1947–1949	Coral	9	–176	72	Hirabayashi et al. 2017
130	29.32	Kikai Island	1901–1947	Coral	6	–200	27	Hirabayashi et al. 2017
144.84	13.60	Guam Island	1939–1949	Coral	72	–153	38	Andrews et al. 2016

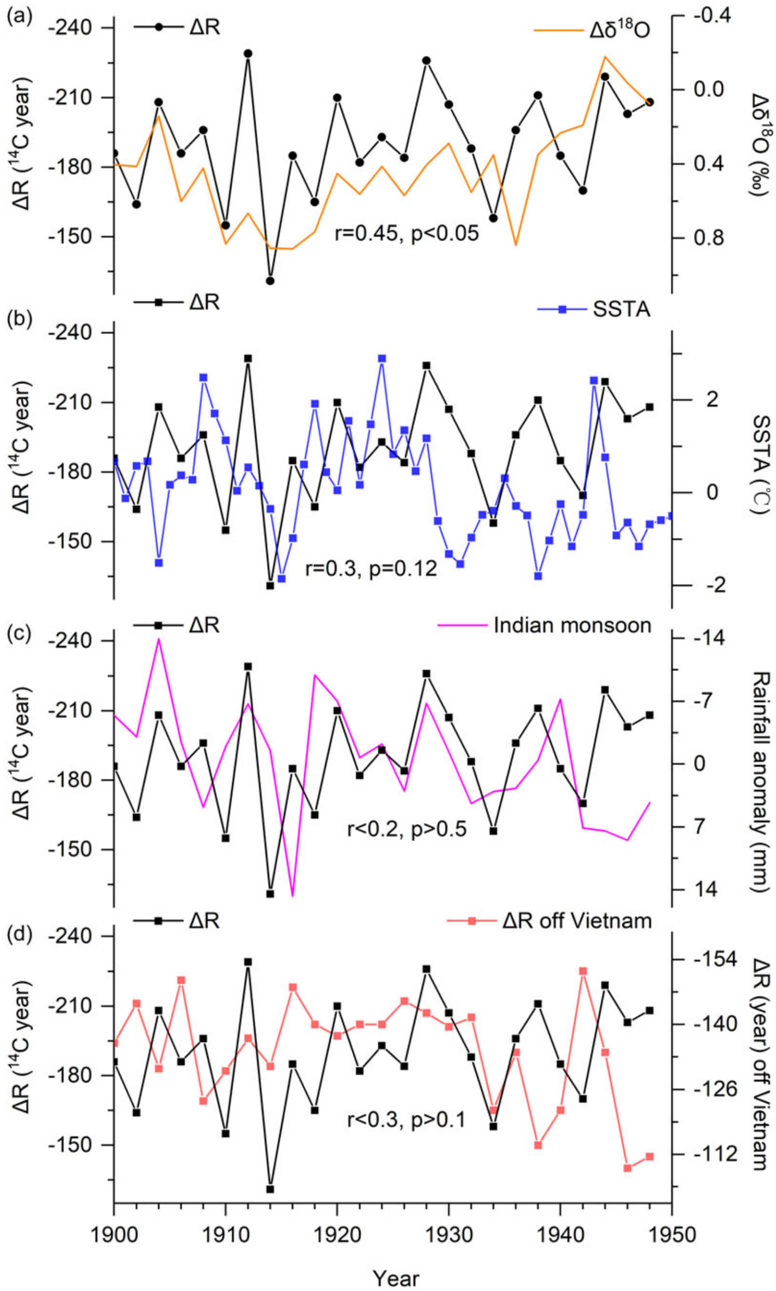

Figure 3. *Comparison of ΔR from Hainan Island with regional climate. (a) comparison of ΔR (black dotted line) with Δδ^{18} O (orange line) from Hainan Island corals (Deng et al. 2017). (b) comparison of ΔR (black dotted line) with SST anomaly (SSTA, blue line) from Hainan Island corals (Liu et al. 2013). (c) comparison of ΔR (black dotted line) with Indian monsoon index (purple line) derived from Indian rainfall anomaly (Singh et al. 2019). (d) comparison of ΔR (red dotted line) off Hòn Tre Island, Vietnam (Bolton et al. 2016) with ΔR (black dotted line) at east Hainan Island.*

difference between Xisha Island and Hainan Island reflects their different oceanographic setting (Hainan Island is a coastal site and Xisha is an open ocean site). Thereby the difference in sampling resolution would exert negligible effect on our ΔR variability. Considering the seasonal climate-

https://doi.org/10.1017/RDC.2024.118 Published online by Cambridge University Press

dominant circulation in the SCS (Hu et al. 2000), we compare indicators of regional climate and corresponding ΔR values to explore possible linkages.

Monsoon rainfall influenced regional ΔR off east Hainan Island

As demonstrated by SST (Wu and Li 2003), nutrient (Hu et al. 2021), climatological Advanced Very High-Resolution Radiometer SST image and numerical model (Jing et al. 2009), wind-induced coastal upwelling at east of Hainan Island has been thoroughly investigated. Thus, ΔR values here are probably controlled by regional upwelling. However, the ΔR from Hainan Island showed poor correlation (Figure 3b, $r=0.3$, $p=0.12$) with reconstructed intensity of regional upwelling based on the summer sea surface temperature anomaly from a 121-yr coral record (Liu et al. 2013). In addition, despite our ΔR values displayed consistent variations with the Indian rainfall anomaly (viewed as intensity of SASM, Singh et al. 2019) in part, insignificant correlation (Figure 3c, $r<0.2$, $p>0.5$) between them did not support the dominant influence from SASM on ΔR off Hainan Island. Therefore, we excludeded the SASM induced wind as a driver for influencing ΔR off Hainan Island.

Significantly, reconstructed regional SASM precipitation index ($\Delta\delta^{18}O$) from Hainan Island correlated well ($r=0.45$, $p<0.05$) with our ΔR (Figure 3 a, Deng et al. 2017), which probably indicated that monsoon rainfall dominated regional ΔR. The minor difference between average ΔR value in Xisha Island (–201±16 ^{14}C years) and Hainan Island (–190±23 ^{14}C years) suggested the underlying effect of runoff/rainfall from Hainan Island, considering that aged seawater vigorously upwelled off Hainan Island. The influence from freshwater, lowering the ΔR values, likely explained the lower average ΔR values than the average ΔR off the coastal site at Hòn Tre Island, Vietnam (Bolton et al. 2016), areas with distinct upwelling activity (Figure 3 d). Furthermore, previous research indicated that both the river plume and coastal upwelling contributed to the carbonate system at east of Hainan according to observation data from 2014 to 2015 (Dong et al. 2017). Lin et al. (2016) suggested that freshwater impacted the northeastern coast of Hainan Island more than the eastern coast of Hainan Island, based on cruise observations and reanalysis data from 2009. Therefore, we proposed that runoff/rainfall dominated the ΔR values off Hainan Island. Further, as part of SASM, wind and precipitation from SASM both have an impact on Hainan Island, the former dominates the upwelling off Hainan Island (Hu and Wang 2016; Li et al. 2012), while the latter regulates the regional ΔR.

As mentioned above, upwelling off Hainan Island held less contribution to variable ΔR, despite the seawater ages still older than the atmospheric. To quantify how the freshwater input contributed to ΔR off Hainan Island, a two end-members model was used as follows.

For convenience, all measured *F* value were employed for the model. We supposed the *F* value of the freshwater runoff was determined from atmospheric *F* value of the same year. The *F* value of the upwelled deepwater was equated with the *F* value of off Hòn Tre Island, Vietnam (Bolton et al. 2016), considering its characteristics with significant upwelling activity. The contribution of the two end-members were computed using Equations (6–7):

$$f_r + f_w = 1 \tag{6}$$

$$F_r f_r + F_w f_w = F_{obs} \tag{7}$$

where f indicates the fractions of runoff or freshwater (f_r), upwelled deepwater (f_w). F_r, F_w, and F_{obs} denote the *F* value of the runoff, the deepwater, and the measured *F* value east of Hainan Island, respectively. Given the negligible difference of DIC between runoff (1805 mol kg^{-1}) and the offshore seawater (1937 mol kg^{-1}, observational data from 2014) (Dong et al. 2017), f_r and f_w are assumed to represent the runoff and deepwater fractions.

The two end-members model results revealed that the f_r varied from 0% to 19.2%, with an average of 11.4%. The calculated runoff proportion correlated well ($r=-0.53$, $p<0.01$) with the local precipitation reconstructed from the coral (Figure S2, see Supplementary) (Deng et al. 2017). This correlation reinforced our two end-members model, despite previous study suggested nearly 50% runoff contribution, as observed from measured pH value (Dong et al. 2017). Hence, ΔR off Hainan Island was mainly dominated by the SASM induced precipitation rather than wind, namely the upwelling activity.

EAWM influenced regional ΔR in Xisha Island

Different from Hainan Island, the oceanographic setting around Xisha Island is not dominated by upwelling. Due to negligible runoff, freshwater input is expected to exert a minor impact on seawater $\Delta^{14}C$. Hence, ΔR values at Xisha Island were dominated by the regional circulation. Lacking observational data, we correlated the Xisha Island ΔR with the reconstructed SST (Sun et al. 2004), precipitation (Han et al. 2019), and wind speed (intensity of EAWM, Song et al. 2012) from Xisha Island corals (Figure 4 a–c). We observed a negative correlation between EAWM and ΔR (with one year lag, $r=-0.37$, $p<0.1$), and an insignificant relationship between ΔR and reconstructed SST ($r<0.1$, $p>0.5$) and precipitation ($r=-0.15$, $p>0.5$). Similarly, the SASM displayed a negligible correlation ($r<0.1$, $p>0.5$) with the ΔR. Therefore, the ΔR in Xisha Island was mainly modulated by the EAWM, the same as the surface circulation in winter.

However, given the Ekman transport, the stronger the wind, the more overturning of the deep water, thus the more negative seawater DIC $\Delta^{14}C$ and higher ΔR values (Druffel and Griffin 1993; Grumet et al. 2004). The abnormal negative correlation here probably reflects horizontal water mass movement. Not unique, a seasonal $\Delta^{14}C$ signal from 1968 to 1995, in Currimao, the Philippines, was found to be positively correlated with winter wind speed, implying horizontal transport from the Luzon Strait (Hirabayashi et al. 2017). Moreover, the winter $\Delta^{14}C$ variations from coral at Houbihu (Ramos et al. 2019) in the 1970s displayed a distinct positive correlation between $\Delta^{14}C$ and EAWM. Despite post-bomb rather than pre-bomb relationship between coral $\Delta^{14}C$ and EAWM was revealed, the positive correlation between coral $\Delta^{14}C$ and EAWM did support the horizontal transport of sea water from the Luzon Strait. This horizontal transport of sea water was consistent with our proposal mentioned above. Furthermore, from the Luzon Strait to the Xisha Island, the ΔR should gradually decrease as a result of keeping exchanging between the seawater and air, as can be seen the ΔR values along the path from the Palaui island (–99±105 ^{14}C years) (Ramos et al. 2019) to Currimao (–142±38 ^{14}C years) (Hirabayashi et al. 2019), and Xisha Island (–201±16 ^{14}C years). Consequently, the strong EAWM would facilitate the transport of surface water from Luzon Strait to Xisha Island, leading to a distinct negative correlation with the ΔR. Likewise, in spite of the long time, the one-year lag of ΔR probably represents the transporting time.

Implication for paleoclimate

As shown in Figure 5, the average ΔR inside the SCS (–161±39 ^{14}C years) is similar to the ΔR on Guam Island (–153±38 ^{14}C years) (Andrews et al. 2016) and Palau Island (–154±21 ^{14}C years) (Glynn et al. 2013). This similarity implies that the water in the SCS originated from the western Pacific (Qu et al. 2009), despite that the Kuroshio Current (KC) furnished the SCS to a large extent and the ΔR along the KC path progressively decreased (Nan et al. 2015; Yoneda et al. 2007). Nevertheless, the ΔR inside the SCS is not uniform. The distribution of regional average ΔR was nearly paralleled with the circulation. From the Luzon Strait to the south SCS, the gradually decreased ΔR probably indicated that the seawater kept exchanging with the air along the current path. In addition, the upwelling area held the larger ΔR due to the upwelled depleted $\Delta^{14}C$ water, like the Hon Tre Island (Bolton et al. 2016). In contrast, supplied by plentiful runoff, the ΔR values from estuary was extremely low, like the minimum ΔR in Con Dao Island (Dang et al. 2004). Additionally, near the Luzon Strait, the regional ΔR ranged from –76±98 to –99±105 ^{14}C years, higher than the ΔR from other sites. Considering the regional bedrock (without limestone) and the special deep circulation across the Luzon Strait, the higher ΔR may

https://doi.org/10.1017/RDC.2024.118 Published online by Cambridge University Press

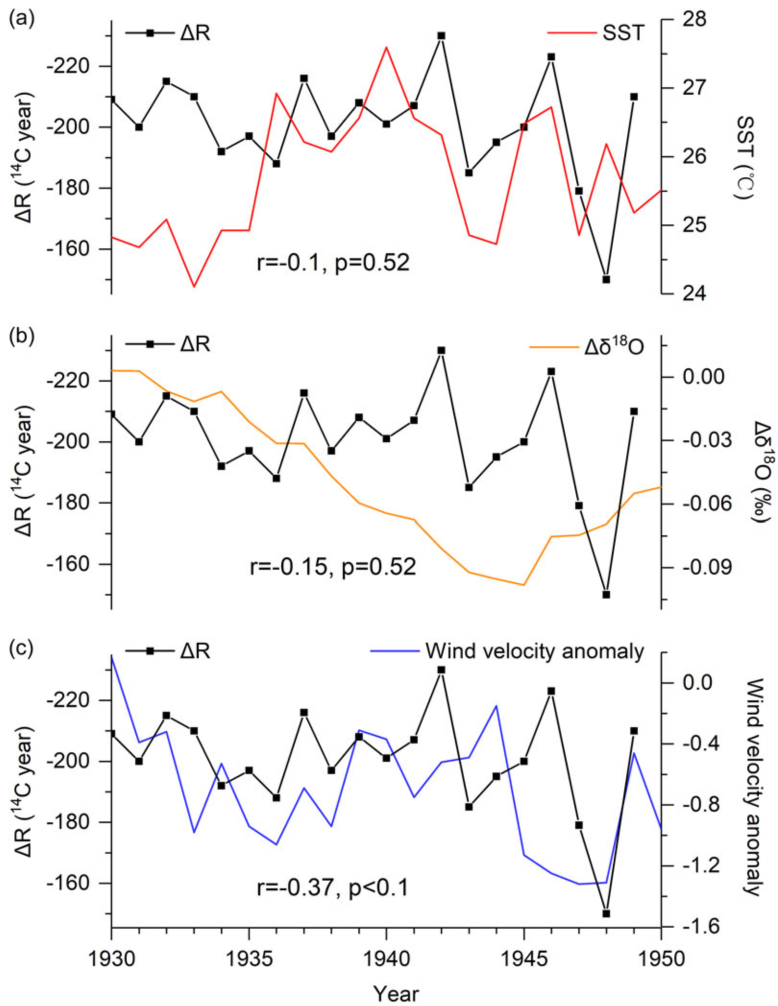

Figure 4. *Comparison of ΔR from Xisha Island with regional climate. (a) comparison of ΔR (black dotted line) in Xisha Island with reconstructed SST (red line) from coral in Xisha Island (Sun et al. 2004). (b) comparison of ΔR (black dotted line) with Δδ^{18}O (orange line) from coral at Yongxing Island (Han et al. 2019). (c) comparison of ΔR (black dotted line) with reconstructed winter wind velocity anomaly (blue line) from coral in Xisha Island (Song et al. 2012). Note that ΔR lagged the wind velocity anomaly by one year.*

be contributed to the overturned deepwater in the Bashi Strait (Qu et al. 2006). Moreover, there seems homogeneous ΔR in the south SCS and northwest SCS, with ΔR of nearly –161±9 ^{14}C years (average of ΔR in Singapore, Saigon and Ko Ang Trang in Thailand) and –194±22 ^{14}C years (average of ΔR in Xisha and Hainan Island), respectively. In summary, the average ΔR of –161±39 ^{14}C years in the SCS was similar to ΔR in the western Pacific. The northwest SCS and estuarine area (such as the Mekong River estuary) were characterized with low ΔR, the Luzon Strait area and the upwelling zone processed high ΔR.

Previous studies indicated that the El Niño Southern Oscillation (ENSO) and the East Asian summer monsoon affected the SCS ΔR values through time, using paired ^{14}C and U-Th dates on pristine corals from the past 8000 years (Hua et al. 2020; Yu et al. 2010). However, in spite of the short duration of our ΔR time series data, our results indicated that the monsoon (like SASM and EAWM) mainly modulated

https://doi.org/10.1017/RDC.2024.118 Published online by Cambridge University Press

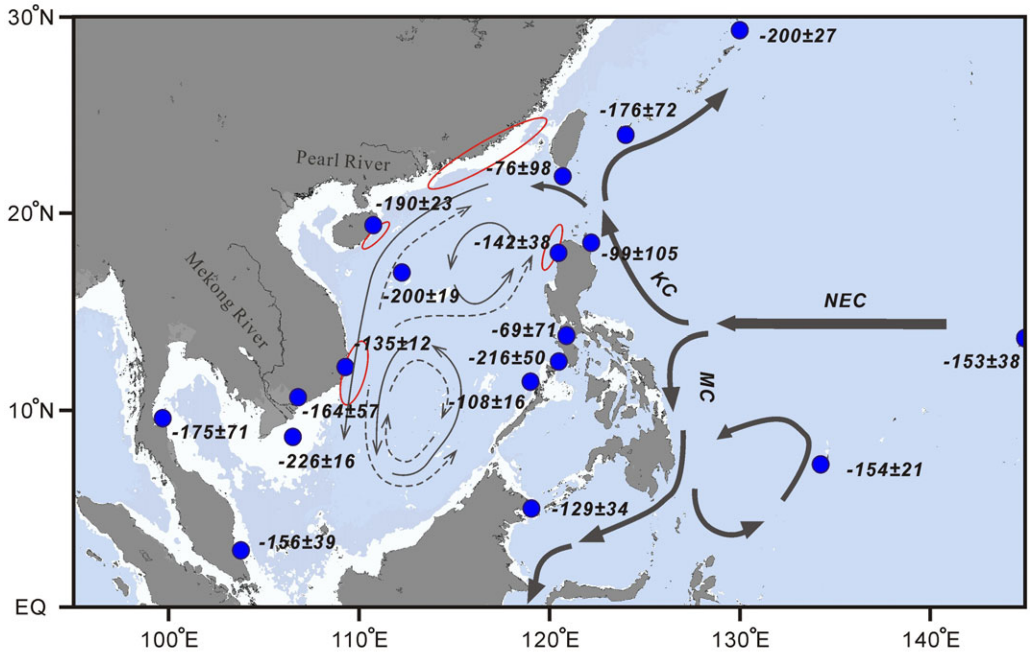

Figure 5. *The distribution of ΔR around the SCS. The ΔR was based on Marine 20 Curve, expressed as regional average ΔR with errors (black symbol). Information of the sites (blue dot) is given in Table 2. The average ΔR for Xisha Island of –200±19 ^{14}C years shown in this figure was calculated using data from this study and from Southon et al. (2002). The red circles denote the coastal upwelling area (Hu and Wang 2016). The thick gray line represents circulation outside the SCS, while the thin gray solid and dashed line represents winter and summer circulation inside the SCS, respectively (Fang et al. 1998). NEC = North Equatorial Current, KC = Kuroshio Current, MC = Mindoro Current.*

the ΔR in the north SCS. Normally, large-scale ΔR variability will be dominated by ocean circulation (Stuiver and Ostlund 1983), with minor effect near estuarine area. These tight relations have been verified from coral Δ^{14}C (Druffel et al. 2014; Fallon and Guilderson 2008; Rafter et al. 2017). In addition, based on the interannual coral Δ^{14}C records from the Luzon Strait, Ramos et al. (2019) highlighted that the monsoon primarily control inside the SCS, while ENSO dominated outside the SCS. Therefore, given the negative correlation between ΔR from Xisha Island and EAWM, the glacial SCS ΔR was probably lower than interglacial period, rather than expected from previous studies (Siani et al. 2001).

Conclusion

Here two corals from the north SCS were studied to reveal temporal ΔR variation and its relationship to climate change. The coral ΔR at east of Hainan Island was modulated by the Southern Asian Summer Monsoon (SASM), which affected the regional runoff, rather than wind induced upwelling. The freshwater from runoff contributed average 11.4% based on the two end-members model. Different from Hainan Island, the coral ΔR at Xisha Island was mainly regulated by the East Asian Winter Monsoon (EAWM), which blew the surface water to Xisha Island along the circulation. Hence the stronger the wind, the lower the ΔR at Xisha Island, especially during glacial, when the EAWM became stronger. The average ΔR in the SCS was –161±39 ^{14}C years, by compiling the radiocarbon data from 1900 to 1950, based on the new calibration curve, Marine20. In spite the limited data, our result from

Xisha Island and Hainan Island together implied that the ΔR was mainly regulated by the monsoon. The newly average ΔR for the SCS would contribute to paleoclimate research in the SCS. Further research is needed for the long-term and seasonal ΔR variety.

Supplementary material. To view supplementary material for this article, please visit https://doi.org/10.1017/RDC.2024.118.

Acknowledgments. This research was supported by the Strategic Priority Research Program of Academy of Sciences (grant No. XDB40000000), the Natural Science Foundation of China (No. 41991252, No. 41706071), the Youth Innovation Promotion Association (No. 2019401). The authors thank great help for this work by the State Key Laboratory of Loess and Quaternary Geology, Institute of Earth Environment, Chinese Academy of Sciences, the Pilot National Laboratory for Marine Science and Technology (Qingdao), and the Ministry of Science and Technology of China. The authors would also like to thank Prof. George Burr for linguistic assistance and Dr. Xuefei Chen for coral sampling.

Declaration of competing interests. The authors declare that they have no known competing financial interests or personal relationships that could have appeared to influence the work reported in this paper.

Reference

Alves EQ, Macario K, Ascough P and Ramsey CB (2018) The worldwide marine radiocarbon reservoir effect: Definitions, mechanisms, and prospects. *Reviews of Geophysics* **56**, 278–305. https://doi.org/10.1002/2017RG000588.

Andrews AH, Asami R, Iryu Y, Kobayashi DR and Camacho F (2016) Bomb-produced radiocarbon in the western tropical Pacific Ocean: Guam coral reveals operation-specific signals from the Pacific Proving Grounds. *Journal of Geophysical Research: Oceans* **121**, 6351–6366. https://doi.org/10.1002/2016JC012043.

Bolton A, Goodkin NF, Druffel ERM, Griffin S and Murty SA (2016) Upwelling of Pacific intermediate water in the South China Sea revealed by coral radiocarbon record. *Radiocarbon* **58**(1), 37–53. https://doi.org/10.1017/RDC.2015.4.

Burr GS, Beck JW, Corrège T, Cabioch G, Taylor FW and Donahue DJ (2009) Modern and Pleistocene reservoir ages inferred from south Pacific corals. *Radiocarbon* **51**(1), 319–335. https://doi.org/10.1017/S0033822200033853.

Butzin M, Kohler P and Lohmann G (2017) Marine radiocarbon reservoir age simulations for the past 50000 years. *Geophysical Research Letters* **44**, 8473–8480. https://doi.org/10.1002/2017GL074688.

Cai S, Liu H and Li W (2002) Water transport exchange between the South China Sea and its adjacent seas. *Advances in Marine Science* (in Chinese) **20**(3), 29–34.

Chen X, Deng W, Kang H, Zeng T, Zhang L, Zhao J and Wei G (2021) A replication study on coral $\delta^{11}B$ and B/Ca and their variation in modern and fossil Porites: implications for coral calcifying fluid chemistry and seawater pH changes over the last millennium. *Paleoceanography and Paleoclimatology* **36**(10). https://doi.org/10.1029/2021PA004319.

Dang PX, Mitsugchi T, Kitagawa H, Shibata Y and Kobayashi T (2004) Marine reservoir correction in the south off Vietnam estimated from an annually-banded coral. *Radiocarbon* **46**(2), 657–660. https://doi.org/10.1017/S0033822200035712.

Deng WF, Liu X, Chen XF, Wei GJ, Zeng T, Xie LH and Zhao JX (2017) A comparison of the climates of the medieval climate anomaly, Little Ice Age, and Current Warm Period reconstructed using coral records from the northern South China Sea. *Journal of Geophysical Research: Oceans* **122**(1), 264–275. https://doi.org/10.1002/2016JC012458.

Deng W, Wei G, Xie L, Ke T, Wang Z, Zeng T and Liu Y (2013) Variations in the Pacific decadal oscillation since 1853 in a coral record from the northern South China Sea. *Journal of Geophysical Research: Oceans* **118**(5), 2358–2366. http://doi.org/10.1002/jgrc.20180.

Dong X, Huang H, Zheng N, Pan A, Wang S, Huo C, Zhou K, Lin H and Ji W (2017) Acidification mediated by a river plume and coastal upwelling on a fringing reef at the east coast of Hainan Island, Northern South China Sea. *Journal of Geophysical Research: Oceans* **122**, 7521–7536. https://doi.org/10.1002/2017JC013228.

Druffel ERM (1997) Geochemistry of corals: proxies of past ocean chemistry, ocean circulation, and climate. *Proceedings of the National Academy of Sciences of the United States of America* **94**(16), 8354–8361. https://doi.org/10.1073/pnas.94.16.8354.

Druffel ERM and Griffin S (1993) Large variations of surface ocean radiocarbon: Evidence of circulation changes in the southwestern Pacific. *Journal of Geophysical Research* **98**(C11), 20249–20259.

Druffel ERM, Griffin S, Glynn DS, Dunbar RB, Mucciarone DA and Toggweiler JR (2014) Seasonal radiocarbon and oxygen isotopes in a Galapagos coral: Calibration with climate indices. *Geophysical Research Letters* **41**(14), 5099–5105. http://doi.org/10.1002/2014GL060504.

Fallon SJ and Guilderson TP (2008) Surface water processes in the Indonesian throughflow as documented by a high resolution coral $\Delta^{14}C$ record. *Journal of Geophysical Research: Oceans* 113. https://doi.org/10.1029/2008JC004722.

Fang G, Fang W, Fang Y and Wang K (1998) A survey of studies on the South China Sea upper ocean circulation. *Acta Oceanographica Taiwanica* **37**(1), 1–16.

Glynn D, Druffel E, Griffin S, Dunbar R, Osborne M and Sanchez-Cabeza JA (2013) Early bomb radiocarbon detected in Palau Archipelago corals. *Radiocarbon* **55**(2–3), 1659–1664. https://doi.org/10.1017/S0033822200048578.

Goodkin NF, Bolton A, Hughen KA, Karnauskas KB, Griffin S, Phan KH, Vo ST, Ong MR and Druffel ERM (2019) East Asian monsoon variability since the sixteenth century. *Geophysical Research Letters* **46**(9), 4790–4798. https://doi.org/10.1029/2019GL081939.

Grottoli AG, Gille ST, Druffel ERM and Dunbar RB (2003) Decadal timescale shift in the ^{14}C record of a central Equatorial Pacific coral. *Radiocarbon* **45**(1), 91–99. http://doi.org/10.1017/S0033822200032422.

Grumet NS, Abram NJ, Beck JW, Dunbar RB, Gagan MK, Guilderson TP, Hantoro WS and Suwargadi BW (2004) Coral radiocarbon records of Indian Ocean water mass mixing and wind induced upwelling along the coast of Sumatra, Indonesia. *Journal of Geophysical Research* **109**, C05003. https://doi.org/10.1029/2003JC002087.

Han T, Yu K, Yan H, Yan H, Tao S, Zhang H, Wang S and Chen T (2019) The decadal variability of the global monsoon links to the north Atlantic climate since 1851. *Geophysical Research Letters* **46**, 9054–9063. https://doi.org/10.1029/2019GL081907.

Heaton TJ, Köhler P, Butzin M, Bard E, Reimer RW, Austin WEN, Ramsey CB, Grootes PM, Hughen KA, Kromer B, Reimer PJ, Adkins J, Burke A, Cook MS, Olsen J and Skinner LC (2020) Marine20-the marine radiocarbon age calibration curve (0–55,000 cal BP). *Radiocarbon* **62**(4), 779–820. http://doi.org/10.1017/RDC.2020.68.

Hirabayashi S, Yokoyama Y, Suzuki A, Esat T, Miyairi Y, Aze T, Siringan F and Maeda Y (2019) Local marine reservoir age variability at Luzon Strait in the South China Sea during the Holocene. *Nuclear Instruments and Methods in Physics Research Section B Beam Interactions with Materials and Atoms* **455**, 171–177. https://doi.org/10.1016/j.nimb.2018.12.001.

Hirabayashi S, Yokoyama Y, Suzuki A, Miyairi Y, Aze T, Siringan F and Maeda Y (2017) Radiocarbon variability recorded in coral skeletons from the northwest of Luzon Island, Philippines. *Geoscience Letters* **4**(15). https://doi.org/10.1186/s40562-017-0081-8.

Hu J, Kawamura H, Hong H and Qi Y (2000) A review on the currents in the South China Sea: seasonal circulation, South China Sea warm Current and Kuroshio Intrusion. *Journal of Oceanography* **56**(6), 607–624. https://doi.org/10.1023/A:1011117531252.

Hu J and Wang XH (2016) Progress on upwelling studies in the China seas. *Reviews of Geophysics* **54**(3), 653–673. https://doi.org/10.1002/2015RG000505.

Hu Q, Chen X, Huang W and Zhou F (2021) Phytoplankton bloom triggered by eddy-wind interaction in the upwelling region east of Hainan Island. *Journal of Marine System* **214**(103470), 1–11. http://doi.org/10.1016/j.jmarsys.2020.103470.

Hua Q, Ulm S, Yu K, Clark TR, Nothdurft LD, Leonard ND, Pandolfi JM, Jacobsen GE and Zhao J (2020) Temporal variability in the Holocene marine radiocarbon reservoir effect for the tropical and south Pacific. *Quaternary Science Reviews* 249. https://doi.org/10.1016/j.quascirev.2020.106613.

Hua Q, Webb GE, Zhao J, Nothdurft LD, Lybolt M, Price GJ and Opdyke BN (2015) Large variations in the Holocene marine radiocarbon reservoir effect reflect ocean circulation and climatic changes. *Earth and Planetary Science Letters* **422**, 33–44. http://doi.org/10.1016/j.epsl.2015.03.049.

Jing ZY, Qi Y, Hua Z and Zhang H (2009) Numerical study on the summer upwelling system in the northern continental shelf of the South China Sea. *Continental Shelf Research* **29**(2), 467–478. https://doi.org/10.1016/j.csr.2008.11.008.

Kang H, Chen X, Deng W, Wang X, Cui H, Liu X, Cai G, Zeng T, Zhao J and Wei G (2021) Skeletal growth response of Porites coral to long-term ocean warming and acidification in the South China Sea. *Journal of Geophysical Research: Biogeosciences* **126**(10). https://doi.org/10.1029/2021JG006423.

Li Y, Peng S, Yang W and Wang D (2012) Numerical simulation of the structure and variation of upwelling off the east coast of Hainan Island using QuikSCAT winds. *Chinese Journal of Oceanology and Limnology* **30**(6), 1068–1081. http://doi.org/10.1007/s00343-012-1275-8.

Lin P, Hu J, Zheng Q, Sun Z and Zhu J (2016) Observation of summertime upwelling off the eastern and northeastern coasts of Hainan Island, China. *Ocean Dynamics* **66**, 387–399. http://doi.org/10.1007/s10236-016-0934-2.

Lisiecki E and Raymo E (2005) A Pliocene-Pleistocene stack of 57 globally distributed benthic $\delta^{18}O$ records. *Paleoceanography* 20, PA1003. https://doi.org/10.1029/2004PA001071.

Liu Q, Jiang X, Xie SP and Liu WT (2004) A gap in the Indo-Pacific warm pool over the South China Sea in boreal winter: seasonal development and interannual variability. *Journal of Geophysical Research* **109**, C07012. https://doi.org/10.1029/2003JC002179.

Liu Y, Peng Z, Shen CC, Zhou R, Song S, Shi Z, Chen T, Wei G and DeLong KL (2013) Recent 121-year variability of western boundary upwelling in the northern South China Sea. *Geophysical Research Letters* **40**, 3180–3183. http://doi.org/10.1002/grl.50381.

McKee BA, Aller RC, Allison MA, Bianchi TS and Kineke GC (2004) Transport and transformation of dissolved and particulate materials on continental margins influenced by major rivers: benthic boundary layer and seabed processes. *Continental Shelf Research* **24**(7–8), 899–926. https://doi.org/10.1016/j.csr.2004.02.009.

Mitsuguchi T, Dang PX, Kitagawa H, Yoneda M and Shibata Y (2007) Tropical South China Sea surface ^{14}C record in an annually banded coral. *Radiocarbon* **49**(2), 905–914. http://doi.org/10.1017/S0033822200042776.

Nan F, Xue H and Yu F (2015) Kuroshio intrusion into the South China Sea: A review. *Progress in Oceanography* **137**, 314–333. https://doi.org/10.1016/j.pocean.2014.05.012.

Oliveira MI, Carvalho C, Macario K, Evangelista H, Lamounier S and Hammerschlag I (2019) Marine reservoir corrections for the Brazilian northern coast using modern corals. *Radiocarbon* **61**(2), 587–597. https://doi.org/10.1017/RDC.2018.145.

Qu T, Girton JB and Whitehead A (2006) Deepwater overflow through Luzon Strait. *Journal of Geophysical Research: Oceans* **111**, C01001. https://doi.org/10.1029/2005JC003139.

Qu T, Song YT and Yamagata T (2009) An introduction to the South China Sea throughflow: Its dynamics, variability, and application for climate. *Dynamics of Atmospheres and Oceans* **47**(1–3):3–14. https://doi.org/10.1016/j.dynatmoce.2008.05.001.

Rafter PA, Sanchez SC, Ferguson J, Carriquiry JD, Druffel ERM, Villaescusa JA and Southon JR (2017) Eastern tropical North Pacific coral radiocarbon reveals North Pacific Gyre Oscillation (NPGO) variability. *Quaternary Science Reviews* **160**, 108–115. http://doi.org/10.1016/j.quascirev.2017.02.002.

Ramos RD, Goodkin NF, Druffel ERM, Fan TY and Siringan FP (2019) Interannual coral $\Delta^{14}C$ records of surface water exchange across the Luzon Strait. *Journal of Geophysical Research: Oceans* **124**(1), 491–505. https://doi.org/10.1029/2018JC014735.

Reimer PJ, Bard E, Bayliss A, Beck JW, Blackwell PG, Bronk Ramsey C, Buck CE, Cheng H, Edwards RL, Friedrich M, Grootes PM, Guilderson TP, Haflidason H, Hajdas I, Hatté C, Heaton TJ, Hoffmann DL, Hogg AG, Hughen KA, Kaiser KF, Kromer B, Manning SW, Niu M, Reimer RW, Richards DA, Scott EM, Southon JR, Staff RA, Turney CSM and van der Plicht J (2013) IntCal13 and Marine13 radiocarbon age calibration curves 0–50,000 years cal BP. *Radiocarbon* **55**(4), 1869–1887. https://doi.org/10.2458/azu_js_rc.55.16947.

Shen X, Hu B, Yan H, Donson J, Zhao J, Li J, Ding X, Li Q, Wang X and Xu F (2022) Reconstruction of Kuroshio intrusion into the South China Sea over the last 40 kyr. *Quaternary Science Reviews* **290**, 1–11. https://doi.org/10.1016/j.quascirev.2022.107622.

Siani G, Paterne M, Michel E, Sulpizio R, Sbrana A, Arnold M and Haddad G (2001) Mediterranean Sea surface radiocarbon reservoir age changes since the last glacial maximum. *Science* **294**(5548), 1917–1920. http://doi.org/10.1126/science.1063649.

Singh D, Ghosh S, Roxy MK and McDermid MK (2019) Indian summer monsoon: Extreme events, historical changes, and role of anthropogenic forcings. *WIREs Climate Change* **10**(2), e571. https://doi.org/10.1002/wcc.571.

Slota PJJ, Jull AJT, Linick TW and Toolin LJ (1987) Preparation of small samples for ^{14}C accelerator targets by catalytic reduction of CO. *Radiocarbon* **29**(2), 303–306. http://doi.org/10.1017/S0033822200056988.

Song S, Peng Z, Zhou W, Liu W, Liu Y and Chen T (2012) Variation of the winter monsoon in South China Sea over the past 183 years: Evidence from oxygen isotopes in coral. *Global and Planetary Change* **98–99**, 131–138. https://doi.org/10.1016/j.gloplacha.2012.08.013.

Southon J, Kashgarian M, Metivier B and Yim WW-S (2002) Marine reservoir corrections for the Indian Ocean and southeast Asia. *Radiocarbon* **44**(1), 167–180. https://doi.org/10.1017/S0033822200064778.

Stuiver M and Ostlund HG (1983) GEOSECS Indian Ocean and Mediterranean radiocarbon. *Radiocarbon* **25**(1), 1–29. https://doi.org/10.1017/S0033822200005270.

Stuiver M, Pearson GW and Braziunas T (1986) Radiocarbon age calibration of marine samples back to 9000 cal yr BP. *Radiocarbon* **28**(2B), 980–1021. https://doi.org/10.1017/S0033822200060264.

Stuiver M and Polach HA (1977) Reporting of ^{14}C data. *Radiocarbon* **19**(3), 355–363. https://doi.org/10.1017/S0033822200003672.

Stuiver M, Reimer PJ and Braziunas TF (1998) High-precision radiocarbon age calibration for terrestrial and marine samples. *Radiocarbon* **40**(3), 1127–1151.

Suess HE (1955) Radiocarbon concentration in modern wood. *Science* **122**(3166), 415–417. https://doi.org/10.1126/science.122.3166.415.

Sun Y, Sun M, Wei G, Lee T, Nie B and Yu Z (2004) Strontium contents of a Porites coral from Xisha Island, South China Sea: A proxy for sea-surface temperature of the 20th century. *Paleoceanography and Paleoclimatology* **19**, A2004. https://doi.org/10.1029/2003PA000959.

Tierney JE, Poulsen CJ, Montanez IP, Bhattacharya T, Feng R, Ford H, Hönisch B, Inglis GN, Petersen SV, Sagoo N, Tabor CR, Thirumalai K, Zhu J, Burls NJ, Foster GL, Goddéris Y, Huber BT, Ivany LC, Turner SK, Lunt DJ, McElwain JC, Mills BJW, Otto-Bliesner BL, Ridgwell A and Zhang Y (2020) Past climates inform our future. *Science* **370**(6517). http://doi.org/10.1126/science.aay3701.

Wang P, Li Q and Tian J (2014) Pleistocene paleoceanography of the South China Sea: Progress over the past 20 years. *Marine Geology* **352**, 381–396, http://doi.org/10.1016/j.margeo.2014.03.003.

Wu RS and Li L (2003) Summarization of study on upwelling system in the South China Sea. *Journal of Oceanography in Taiwan Strait* **22**(2), 269–277. (in Chinese with English abstract).

Wu Y and Fallon SJ (2020) Prebomb to Postbomb ^{14}C history from the west side of Palawan Island: Insights into Oceanographic changes in the South China Sea. *Journal of Geophysical Research: Oceans* 125, e2019JC015979. https://doi.org/10.1029/2019JC015979.

Yan H, Liu C, Zhang W, Li M, Zheng X, Wei G, Xie L, Deng W, Sun L (2017) ENSO variability around 2000 years ago recorded by Tridacna gigas $\delta^{18}O$ from the South China Sea. *Quaternary International* **452**, 148–154. https://doi.org/10.1016/j.quaint.2016.05.011.

Yoneda M, Uno H, Shibata Y, Suzuki R, Kumamoto Y, Yoshida K, Takenori S, Atsushi S and Hodaka K (2007) Radiocarbon marine reservoir ages in the western Pacific estimated by pre-bomb molluscan shells. *Nuclear Instruments and Methods in Physics Research Section B: Beam Interactions with Materials and Atoms* **259**(1), 432–437. https://doi.org/10.1016/j.nimb.2007.01.184.

Yu K (2012) Coral reefs in the South China Sea: Their response to and records on past environmental changes. *Science China Earth Sciences* **55**(8), 1217–1229.

Yu K, Quan H, Zhao J, Hodge E, Fink D and Barbetti M (2010) Holocene marine ^{14}C reservoir age variability: Evidence from ^{230}Th-dated corals in the South China Sea. *Paleoceanography* 25:PA3205. https://doi.org/10.1029/2009PA001831.

Yu K, Zhao J, Shi Q, Chen T, Wang P, Collerson KD and Liu T (2006) U-series dating of dead porites corals in the South China Sea: evidence for episodic coral mortality over the past two centuries. *Quaternary Geochronology* **1**(2), 129–141. https://doi.org/10.1016/j.quageo.2006.06.005.

Zeng L, Wang D, Chen J, Wang W and Chen R (2016) SCSPOD14, A South China Sea physical oceanographic dataset derived from in situ measurements during 1919–2014. *Scientific Data* **3**, 160029. http://doi.org/10.1038/sdata.2016.29.

Zhang J, Wang DR, Jennerjahn T and Dsikowitzky L (2013) Land-sea interactions at the east coast of Hainan Island, South China Sea: A synthesis. *Continental Shelf Research* **57**, 132–143. https://doi.org/10.1016/j.csr.2013.01.004.

Zhang P, Xu J, Beil S, Holbourn A, Kuhnt W, Li T, Xiong Z, Yan H, Cui R, Liu H and Wu H (2021) Variability in Indonesian throughflow upper hydrology in response to precession-induced tropical climate processes over the past 120 kyr. *Journal of Geophysical Research: Oceans* **126**, 1–17. https://doi.org/10.1029/2020JC017014.

Zhou W, Zhao X, Lu X, Liu L, Wu Z, Cheng P, Zhao W and Huang C (2016) The 3MV Multi-Element AMS in Xi'an, China: Unique features and preliminary tests. *Radiocarbon* **48**(2), 285–293. http://doi.org/10.1017/S0033822200066492.

Cite this article: Yang L, Zhou W, Cheng P, Zhang L, Wei G, Ma X, Zhou J, Yan H, Chen N, and Hou Y. Monsoon-regulated marine carbon reservoir effect in the northern South China Sea. *Radiocarbon*. https://doi.org/10.1017/RDC.2024.118